Accurate 2D-Momentum-Microscopy-Data Distortion Correction Method for Characterization of Valence Band Spin Polarization

F. Matsui[1,2], Y. Sato[1,2], K. Hagiwara[1], S. Tanaka[3] and S. Suga[3]
[1]*UVSOR Synchrotron Facility, Institute for Molecular Science, Okazaki 444-8585, Japan*
[2]*The Graduate University for Advanced Studies (SOKENDAI), Okazaki 444-8585, Japan*
[3]*SANKEN, The University of Osaka, Ibaraki 567-0047, Japan*

Combining a two-dimensional (2D) spin filter with a photoelectron momentum microscope (PMM) allows multi-channel detection of spin polarization data in 2D momentum and real spaces. An established method for spin polarization analysis is to measure the difference between two patterns taken at the different scattering energies corresponding to the opposite spin-dependent reflectivity [1]. On the other hand, the PMM installed at BL6U in UVSOR [2] is equipped with a spin rotator that flips the direction of the in-plane spin component by ±90°. In addition to the conventional method of taking the scattering energy dependence, the spin rotator makes it possible to detect the spin polarization pattern using a single-scattering-energy condition [3]. The spin rotator can alternate between positive and negative spin polarization detection in times less than one second, opening the door to the efficient accumulation of multi-dimensional (*kz* dispersion, position scan, time evolution, photon polarization, etc.) spin-polarized spectral data. The drawback is that the spin components rotate by ±90° due to Larmor precession in the spin rotator, and the 2D projection distributions also rotate by ±45° due to the Lorentz force simultaneously. To obtain a differential pattern of the 2D distribution of positive and negative spins, the coordinates of the two ±45° rotated patterns must be precisely rotated back to their original orientation to eliminate aberration and distortion.

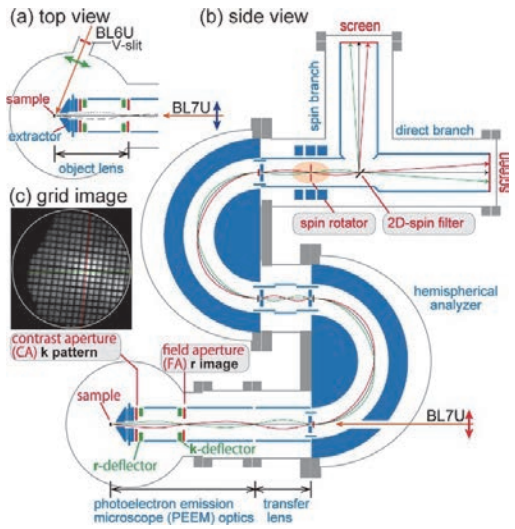

Fig. 1. (a) Top and (b) side views of the photoelectron momentum microscope. (c) The grid inserted at the location of the CA imaged by the direct branch screen.

The PMM at BL6U consists of a six-axes sample stage, PEEM optics, two concentric hemispherical analyzers, a spin rotator, a 2D spin filter, and 2D projection-type detectors in direct and spin-resolved branches as shown in Fig. 1(a) and (b). Instead of a contrast aperture and a field aperture, square grids that can be inserted in the diffraction and back focal planes, respectively, are used to correct distortions of the 2D pattern on the final detection screen. Figure 1(c) shows the image of such a grid on a direct branch screen inserted at the contrast aperture position. Note that the grid is intentionally rotated approximately 5° counter-clockwise to be offset from the pixel array of the CMOS detector.

Figure 2(a) and (b) show images of the CA grid using the ±45° rotation modes of the spin rotator by the direct branch. The latter image is rotated -90° with respect to the former. Figures 2(c) and (d) show the images after numerical correction of coordinate rotation and distortion. As shown in Fig. 2(e) and (f), the horizontal and vertical intensity profiles of the two images (blue: +45°, red: -45° rotation mode) match exactly. Since the spin rotator only affects the photoelectron trajectory after they leave the second hemispherical analyzer, the positional relationship between the valence band pattern and the grid image is not affected. Based on this correction procedure, two spin polarized images are aligned exactly the same coordinates and the spin-polarized valence band dispersion and Fermi surface data are analyzed [3].

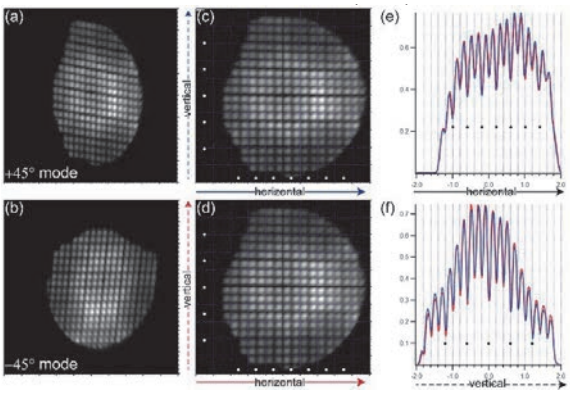

Fig. 2. (a, b) Raw and (c, d) coordinate-corrected grid images of the spin rotator ±45° modes. (e, f) Intensity profiles along the horizontal and vertical directions.

[1] C. Tusche *et al.*, Ultramicroscopy **159** (2015) 520.
[2] F. Matsui *et al.*, J. Phys. Soc. Jpn. **59** (2020) 067001.
[3] F. Matsui *et al.*, submitted (2025).

BL6U

Steady Development of the SP-PMM at UVSOR BL6U with Reliable Data Acquisition and Very High Efficiency

S. Suga[1]

[1]*SANKEN, Osaka University, Mihogaoka, Ibaraki, Osaka 567-0047, Japan*

In order to overcome various and serious difficulty of the single channel spin-resolved-ARPES (SP-ARPES) detection by use of a single hemispherical electron energy analyzer, much more reliable and orders of magnitude higher detection efficiency spin-resolved Photoelectron Momentum Microscope (SP-PMM) with double hemispherical electron energy analyzers (DHDAs) and PEEM type objective lens as well as two dimensional spin detector (SP-PMM) was introduced to UVSOR in 2022.

Two dimensional(2D) real space $E_B(x, y)$ is first measured with changing the sample position and the high quality homogeneous (x, y) regions (even down to 10μm) are selected. Then objective lens mode is switched to the $E_B(k_x, k_y)$ mode and their 2D patterns beyond the 1st Brillouin zone of most materials are recorded at various E_B with 2D detector without sample movement (Fig.1). Even in the case of multidomain cleaved surfaces, PEEM can select a certain particular domain region with the size larger than ~10μm. Then $E_B(k_x, k_y)$ series are integrated as functions of hν. The spatial resolution is decided by the PEEM aperture as good as 50nm. Temperature dependent PMM is feasible down to 10 K now in UVSOR BL6U. The measurements have so far been performed on variety of samples [1-3]. Since the selection rule must be taken into account for understanding several experimental results, we also realized the feasibility of the normal incidence excitation from the branched line of BL7U as shown partly in Publications.

For the spin measurement, Ir(001) clean surface has been so far utilized. This spin filter was used at around 30 eV photoelectron collision with the Ir of the life time of less than 1 day, by use of the spin rotator. Since the tuning of the collision energy down to 10eV became feasible recently after solving an instrumental problem, we will soon start the Au monolayer covered Ir spin filter in few months. Its life time is already checked to be several months. Then we will perform most experiments by this performance-upgraded SP-PMM on the materials under various hot discussions.

So far we have measured the samples with the clean surface prepared either 1) by ion sputtering and annealing or 2) cleaved by peeling off tapes. The 3) pin post pressed cleavage was also employed for wide variety of samples. In addition, the knife-edge cleavage is required for hard materials. So I designed 4) a cleavage crystal recovering box with the knife edge on it. Further the 5) flexibly adjustable knife edge cleavage system is planned to be added in the near future for much more sample cleavage.

In addition, I am preparing an operation manual to use the complex SP-PMM in UVSOR in English, since the demand from the foreign users are expected to increase dramatically in 2025 after the perfect performance of the Au/Ir(001) spin filter, and the use of flexible cleavage system.

Since the normal incidence synchrotron radiation use is very limited, I hope to introduce switchable low energy laser with variable light polarization to be set in the normal incidence configuration. If the pulsed laser is set pump-probe SP-PMM may become feasible.

The collaboration have been so far performed with the research members Prof. F. Matsui, Prof. S. Kera, Dr. Y. Sato, Dr. R. Sagehashi, Dr. K. Hagiwara in UVSOR, IMS & Prof. S. Tanaka, SANKEN, Osaka Univ. I hope to contribute to future works for the next 20 years.

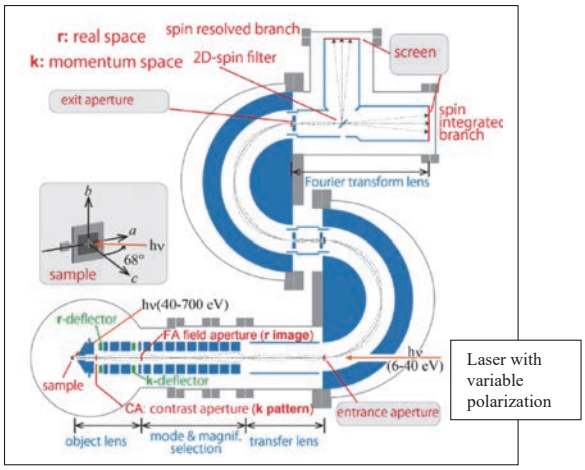

Target is to realize the best resolutions in x, y, k_x, k_y, k_z, Spin (Psx, Psy, Psz) from VUV to Hard X-ray region. Operand measurements are also planned. Spin rotator is in work.

Related-Publication

[1] F. Matsui, K. Hagiwara, E. Nakamura, T. Yano, H. Matsuda, Y. Okano, S. Kera, E. Hashimoto, S. Koh, K. Ueno, T. Kobayashi, E. Iwamoto, K. Sakamoto, S. Tanaka and S. Suga Rev. Sci. Instrum. **94** (2023) 083701.

[2] F. Matsui, K. Hagiwara, Y. Sato, E. Nakamura, R. Sagehashi, S. Kera and S. Suga, Synchrotron Rad. News, **37** (2024).

[3] Y. Higuchi, R. Itaya, H. Saito, T. Toichi, T. Kobayashi, M. Tomita, S. Terakawa, K. Suzuki, K. Kuroda, T. Kotani, F. Matsui, S. Suga, H. Sato, K. Sato and K. Sakamoto, Vacuum, **233** (2025) 113944.

BL6U

Three-Dimensional Fermi Surface Measurement of the Au Crystal Via the Photon-Energy-Dependent Angle-Resolved Photoelectron Spectroscopy Using the Photoelectron Momentum Microscope

S. Tanaka[1], S. Suga[1], K. Hagiwara[2], Y. Sato[2] and F. Matsui[2]
[1]*SANKEN, The University of Osaka, Mihogaoka 8-1, Ibaraki 567-0047, Japan*
[2]*UVSOR Synchrotron Facility, Institute for Molecular Science, Okazaki 444-8585, Japan*

The Fermi surface is a fundamental concept in solid-state physics, representing the boundary in momentum space that separates occupied from unoccupied electronic states. While much progress has been made in understanding the 2D Fermi surface by the angle-resolved photoelectron spectroscopy (ARPES) for materials like thin films or surfaces, obtaining the full 3D Fermi surface has remained a significant challenge, due in part to the complexity of the experimental techniques involved and the immense volume of data required to map the surface in three dimensions.

The dual-beamline photoelectron momentum microscope (PMM) developed at UVSOR is a powerful tool not only for comprehensively characterizing orbital contributions in the electronic structure, but also for determining the Fermi surface, thanks to its high efficiency and extensive momentum-space detection range [1,2]. In recent years, we have been developing methods for 3D Fermi surface determination, both experimentally and through computer-based analyses.

Figure 1 presents the photoelectron intensity maps obtained with the measurements using the PMM for the Au(111) surface, which correspond to the Fermi surface in various planes within the reciprocal lattice space of the Au crystal. Panel (a) shows the k_x–k_y plane at the indicated k_z values, while panels (b) and (c) depict k_y–k_z and k_x-k_z planes at k_x=0 and k_y=0, respectively. The k_z values were estimated using the free-electron final-state model, as

$$k_z = \sqrt{\frac{2m_e}{\hbar^2}(E_k \cos^2\theta + V_0)}$$

where E_k and θ are the kinetic energy and the polar emission angle of the photoelectron, respectively. We assumed the inner potential V_0 is 10.5 eV. Photon energies ranging from 45 eV to 100 eV were employed. Because the Au crystal has three-fold symmetry along the <111> axis, all the intensity distributions in Figs. 1 are the results of averaging over three images; the original distribution and those rotated by 120° and 240°; in order to improve statistics and to suppress the effects of photon polarization. It should be noted that generating the 3D volume data (whose cross sections are shown in Figs. 1) from a series of photon-energy–dependent ARPES measurements required the development of specialized data conversion programs using the cutting-edge AI technique.

In Fig. 1(a), small circles with a radius of approximately 0.17 Å^{-1} around the origin are visible at all k_z values. Additionally, regular hexagons of uniform size, each with an approximate radius of 1 Å^{-1}, are clearly visible in the k_z range of 4.87–4.35 Å^{-1}. As these features do not depend on k_z in terms of their shapes (though their intensity may vary with photon energy), we attribute them to the Au(111) surface states. Other features, which change with k_z, should be attributed to photoelectrons emitted from the bulk 3D-Fermi surface. We are currently developing detailed comparisons between the experimental results and density functional theory (DFT) calculations performed using Quantum Espresso package (version 7.2). While some experimentally observed features are well reproduced by the theoretical calculations, significant discrepancies remain at this stage. Further investigation will be required to refine the methodology for revealing the 3D Fermi surface by exploiting photon-energy–dependent measurements, including the adoption of a more accurate final-state model beyond the free-electron approximation that has been recently proposed [3].

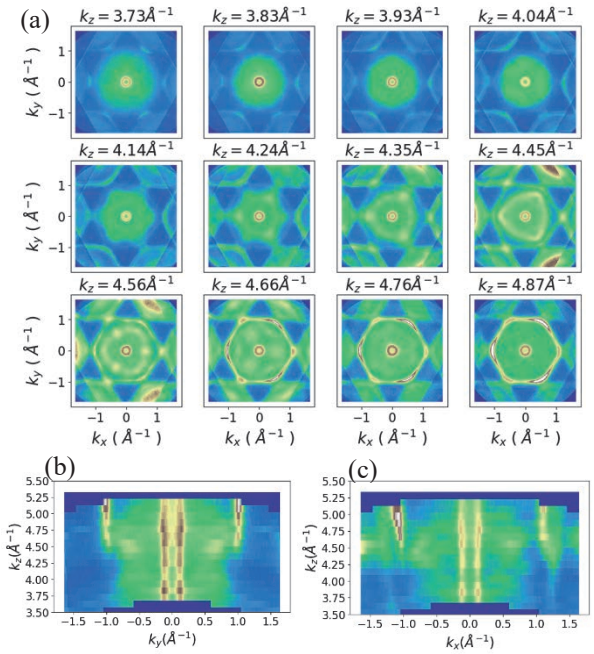

Fig. 1. Photoelectron intensity maps at the Fermi level of Au(111) for various planes in the reciprocal lattice space.

[1] F. Matsui *et al.*, Rev. Sci. Instrum. **94** (2023) 083701.
[2] K. Hagiwara *et al.*, J. Synchrotron Radi. **31** (2024) 540.
[3] V. N. Strocov *et al.*, Nat Commun. **14** (2023) 4827.

BL6U

Photoelectron Momentum Microscopy Study of Termination-Dependent Electronic Structure in $PtBi_2$

Y. Morita[1], K. Nakayama[1], T. Kato[2], S. Souma[2,3], S. Masaki[4], T. Ikushima[4], Y. Moriyasu[4], K. Hagiwara[5], F. Matsui[5], T. Takahashi[1], K. Kudo[4] and T. Sato[1,2,3,6,7]

[1]*Department of Physics, Tohoku University, Sendai 980-8578, Japan*
[2]*Advanced Institute for Materials Research (WPI-AIMR), Tohoku University, Sendai 980-8577, Japan*
[3]*Center for Science and Innovation in Spintronics (CSIS), Tohoku University, Sendai 980-8577, Japan*
[4]*Department of Physics, Graduate School of Science, Osaka University, Toyonaka 560-0043, Japan*
[5]*UVSOR Synchrotron Facility, Institute for Molecular Science, Okazaki 444-8585, Japan*
[6]*International Center for Synchrotron Radiation Innov1ation Smart (SRIS), Tohoku University, Sendai 980-8577, Japan*
[7]*Mathematical Science Center for Co-creative Society (MathCCS), Tohoku University, Sendai 980-8578, Japan*

The discovery of exotic quantum phenomena, such as the half-integer quantum Hall effect in graphene and surface Dirac states in topological insulators, has sparked significant interest in condensed matter physics. These effects originate from novel quasiparticles associated with band degeneracies. For instance, graphene hosts two-dimensional Dirac fermions with linear band dispersion that intersect at a single point, because of the chiral symmetry of its honeycomb lattice. In topological insulators, surface conduction is driven by spin-polarized Dirac fermions, which are protected by time-reversal symmetry and nontrivial bulk topology. These findings stimulate research in exploring quasiparticles beyond Dirac fermions. Among these, Weyl fermions, 3D spin-polarized counterparts of Dirac fermions, are notable for their topological stability and unconventional phenomena such as the chiral anomaly and Fermi arc surface states. Weyl fermions can emerge when either spatial inversion or time-reversal symmetry is broken.

Among candidate Weyl semimetals, $PtBi_2$ is particularly intriguing. It consists of Bi-Pt-Bi trilayer sheets which stack along the c axis. One Bi layer is flat and the other is buckled, resulting in an A-B-C stacking sequence that naturally breaks inversion symmetry. This symmetry breaking combined with strong spin-orbit coupling from the heavy atomic masses lifts spin degeneracy in the band structure. DFT calculations predict that $PtBi_2$ hosts twelve Weyl fermions near $k_z = \pm 0.5\ \pi/c$. Moreover, this material exhibits bulk superconductivity at 0.6 K, and recent studies have suggested the existence of surface superconductivity at a significantly higher temperature (~10 K). This makes $PtBi_2$ a rare platform for exploring the interplay between Weyl fermions and superconductivity at relatively high temperatures. Such coupling could trigger the emergence of topological superconductivity with Majorana fermions, which are their own antiparticles.

In this study, we aimed to gain a comprehensive understanding of the surface-termination-dependent fermiology of $PtBi_2$. We performed photoelectron momentum microscopy measurements at BL6U and mapped the band structure over a wide momentum space. The Fermi surfaces observed for different terminations [Figs. 1(a) and 1(b)] show complex features. Spectral components common to both terminations are attributed to bulk states, while the different features are interpreted as surface states. By comparing our data with DFT-based Fermi surface calculations, we identify signatures of Fermi arc surface states, supporting the Weyl semimetal character of $PtBi_2$.

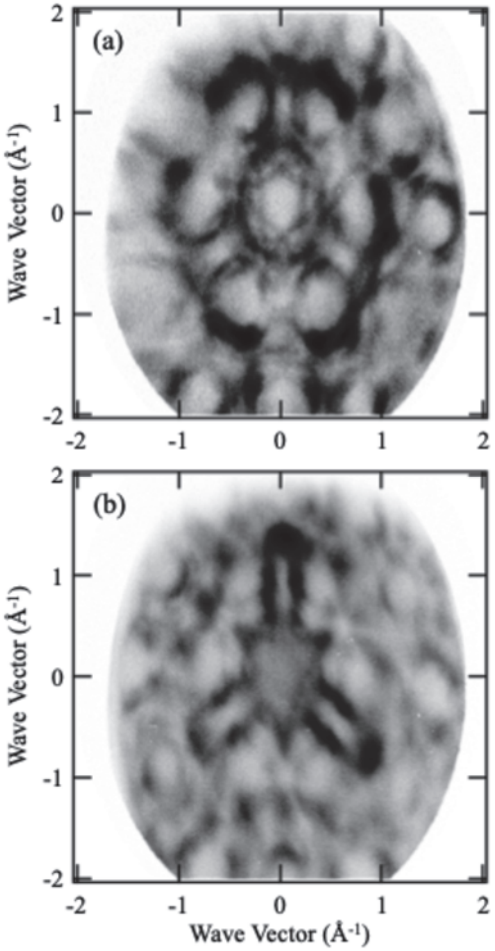

Fig. 1. (a) and (b) Two-dimensional ARPES intensity maps at a constant energy measured on different surface terminations in $PtBi_2$.

BL6U

Momentum-Resolved Resonant Photoelectron Spectroscopy of Au(111) Toward Distinguishing p and d Orbital Contributions

K. Hagiwara[1], R. Sagehashi[1], Y. Sato[1,2], S. Tanaka[3], S. Suga[3] and F. Matsui[1,2]
[1]*UVSOR Synchrotron Facility, Institute for Molecular Science, Okazaki 444-8585, Japan*
[2]*The Graduate University for Advanced Studies (SOKENDAI), Okazaki 444-8585, Japan*
[3]*SANKEN, The University of Osaka, Mihogaoka 8-1, Ibaraki 567-0047, Japan*

Dual-beamline photoelectron momentum microscope (PMM) developed at UVSOR is a powerful tool for comprehensive characterization of orbital contribution to the electronic structure [1, 2]. Normal-incident VUV light from BL7U can be used to analyze atomic orbital symmetry [2]. Resonant photoelectron spectroscopy, utilizing photon-energy ($h\nu$) tunable soft X-ray from BL6U at specific core absorption edges, can provide element- and/or orbital-selective information [3]. We have determined 6p orbital arrangement in the Fermi surface of Au(111) by using horizontally and vertically polarized light from BL7U [2]. However, 5d orbital contribution to the Fermi surface was reported [4]. Therefore, light polarization dependent measurement distinguishing the p and d orbitals is challenging. Here, we have investigated the 6p and 5d orbital contributions to the Fermi surface of Au(111) by resonant photoelectron spectroscopy. Whether the 5d signal selectively enhanced when excited with the photon energy corresponding to transition from 4f to 5d was our question.

Figure 1 shows the photoemission intensity in the valence band region integrated over all momentum as a function of photon energy. One can find noticeable intensity peaks indicated by two dotted lines. These peak lines originate from the Au $4f_{7/2}$ and $4f_{5/2}$ core levels excited by the second order light. Figures 2(a) and 2(b) show the momentum map at E=E_F-0.2eV excited under the resonant ($h\nu$ = 83.9 eV, corresponding to the transition from 4f to 5d) and off-resonant ($h\nu$ = 85 eV) condition, respectively. One can see the bulk state corresponding to the cross section of the Fermi sphere of the bulk Au crystal: the nearly hexagonal contour centered at the $\bar{\Gamma}$ point. The Shockley surface state is centered at the $\bar{\Gamma}$ point as a small circular contour. The corresponding band dispersions are shown in Fig. 2 (d) and 2(e). For comparison, we chose the data taken at these photon energies and the binding energy to avoid influence of the core-level peaks excited by the second order light. As seen from their subtraction in Fig. 2(c) and 2(f), the intensity enhancement under the resonant condition was estimated to be less than 5%. We were not able to find the momentum dependence and different behavior of bulk and surface states for the intensity enhancement. From these results, we cannot conclude the 5d orbital contribution to the Fermi surface of Au(111).

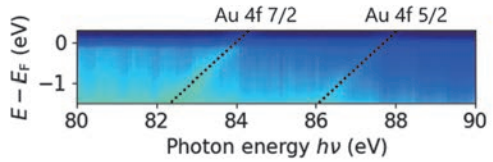

Fig. 1. Photoemission intensity of Au(111) in the valence band region integrated over all momentum as a function of photon energy. Dotted lines indicate the position of for Au $4f_{7/2}$ and $4f_{5/2}$ core levels excited by the second order light.

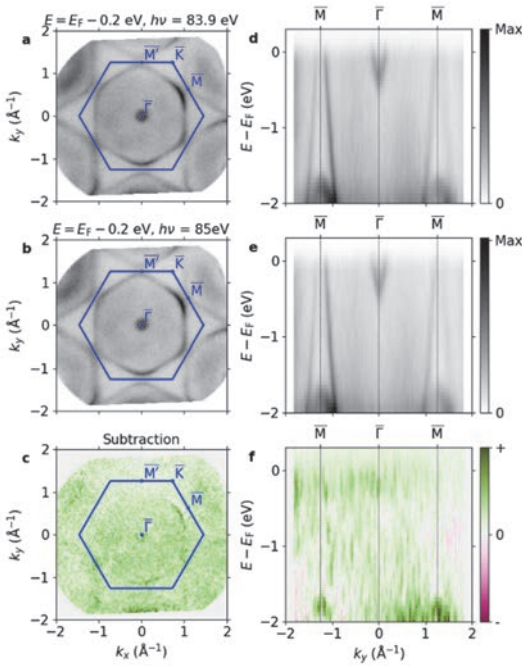

Fig. 2. Momentum-resolved resonant photoelectron spectroscopy of Au(111). (a, b) Momentum distribution at E=E_F-0.2eV excited under the resonant ($h\nu$ = 83.9 eV, corresponding to transition from 4f to 5d) (a) and off-resonant ($h\nu$ = 85 eV) conditions(b). (c) Subtraction between (a) and (b). (d-f) Same as (a-c), but the corresponding band dispersion.

[1] F. Matsui *et al.*, Rev. Sci. Instrum. **94** (2023) 083701.
[2] K. Hagiwara *et al.*, J. Synchrotron Rad. **31** (2024) 540.
[3] F. Matsui *et al.*, J. Phys. Soc. Jpn. **90** (2021) 124710.
[4] A. Sekiyama *et al.*, New J. Phys. **12** (2010) 043045.

Conduction Band of Single Crystal Graphite Embedded in Photoemission Energy-Loss Electrons Visualized by Photoelectron Momentum Microscope

F. Matsui[1], R. Sagehashi[2] and Y. Sato[1]

[1]*UVSOR Synchrotron Facility, Institute for Molecular Science and School of Physical Sciences, The Graduate University for Advanced Studies (SOKENDAI), Okazaki 444-8585, Japan*

[2]*Department of Photo-Molecular Science, Institute for Molecular Science, Okazaki 444-8585, Japan*

The interaction of secondary electrons (SEs) with the conduction band in the photoemission process reduces the emission intensity into the vacuum and produces a negative conduction band pattern contrast [1,2]. This process is very similar to the generation of negative photoelectron diffraction patterns observed in the angular distribution of energy-loss electrons accompanying core-level photoelectron excitation [3]. This means that the same setup as a standard photoelectron spectroscopy system for the characterization of occupied states can be used to visualize the electron-unoccupied conduction band.

Photoelectron momentum microscopy is a suitable system to measure comprehensive band dispersion structure in multiple dimensions (*kx*, *ky*, *kz*, *E*). Here we show that the conduction band of graphite are embedded in the angular and energy distribution of SEs. In addition, the experiment was performed in single-bunch mode, which has a photon flux one order of magnitude lower than the conventional multi-bunch mode. Since the SE intensity is very strong, low photon flux conditions are rather suitable for measuring such bulk crystal conduction band dispersion.

Figure 1(a) shows the overall dispersion of the valence band of graphite. Darker features correspond to directions of larger photoelectron signals. The photon energy was set to 68 eV to match the bulk L symmetry point. The selective detection of photo-electrons from a terrace with a single type of termination confirms that L and L' are not equal, as shown in Figure 1(b) [4]. At the binding energy (BE) of 2.8 eV, the triangles around point K touch each other at point L but are separated at point L'.

Figure 1(c) shows the momentum- resolved kinetic energy distribution of SE electrons. The unoccupied band dispersion appeared as a negative contrast due to the photoelectron absorption process by the conduction band states. Figure 2(d) shows a series of angular patterns at several kinetic energies. The key finding here is that most of the patterns appear with six-fold symmetry, but at kinetic energies of about 20 eV, the patterns become three-fold symmetric. The mechanism by which the three-fold symmetric structure of the top surface of graphite affects the conduction band remains an open question.

[1] V. N. Strocov *et al.* Phys. Rev. B **63** (2001) 205108.
[2] T. Takahashi *et al.*, Phys. Rev. B **32** (1985) 8317.
[3] F. Matsui *et al*., J. Phys. Soc. Jpn. **81** (2012) 013601.
[4] F. Matsui and S. Suga, Phys. Rev. B **105** (2022) 235126.

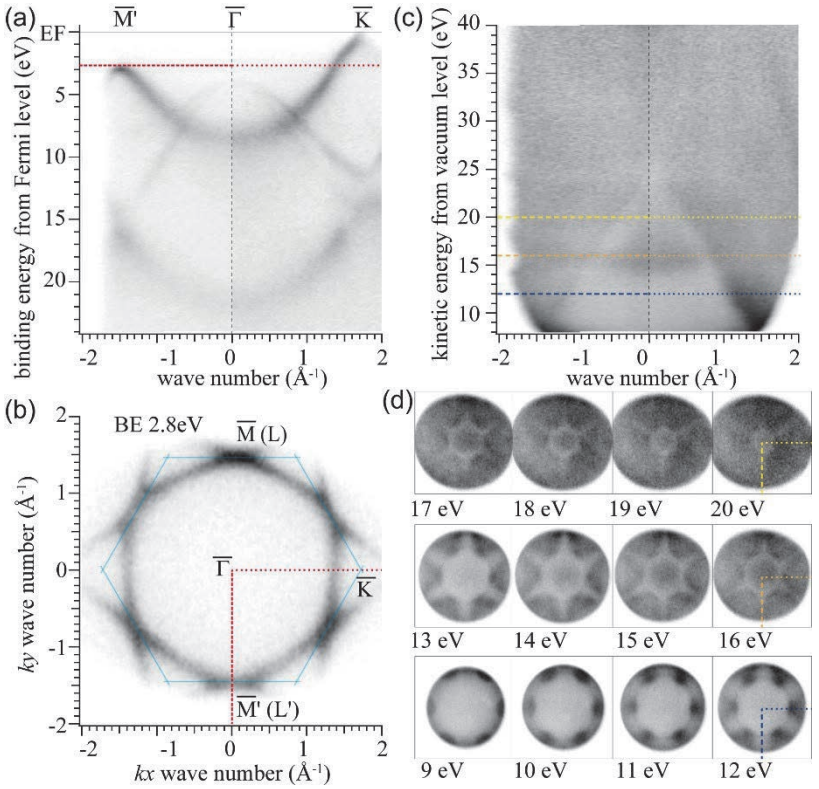

Fig. 1. (a) The overall dispersion of the valence band of graphite. Darker features correspond to directions of larger photoelectron signals. (b) Momentum distribution at the binding energy of 2.8 eV. A red line in (a) corresponds to that in (b). (c) The momentum-resolved kinetic energy distribution of SE electrons. The conduction band signature appears as a lighter grey contrast. (d) A series of SE momentum patterns at several kinetic energies. Note that at kinetic energies of 19 and 20 eV, the patterns appear as three-fold symmetric.

BL6U

Photoelectron Momentum Maps of MnPc on Single Crystal Graphite

R. Sagehashi[1], Y. Sato[2], F. Matsui[2] and S. Kera[1,2]
[1]*Department of Photo-Molecular Science, Institute for Molecular Science, Okazaki 444-8585, Japan*
[2]*UVSOR Synchrotron Facility, Institute for Molecular Science, Okazaki 444-8585, Japan*

Metal complex molecules form ligand fields, which resolve *d*-orbital degeneracy of their metal atoms. Metal-phthalocyanine (MPc) has planar structure and a transition metal atom is located at the center (shown in the inset of Fig. 1). Since MPc molecules are stacked on top of each other via π-π interaction, the ligand field is also formed between layers [1]. Therefore, the electronic and spin state is affected by the film formation significantly.

In this study, we investigated the influence of Mn-phthalocyanine (MnPc) adsorption and film formation on its electronic state by using photoelectron momentum microscopy (PMM) at BL6U. Here, single crystal graphite (SCG) for the substrate was cleaved in vacuum ($< 9.90\times10^{-8}$ Pa). MnPc was in-situ deposited ca. 6.0 Å by deposition rate of 0.30 Å/min measured by quartz crystal microbalance. In this PMM experiment, incoming light had photon energy of 54.0 eV and incident with 68° to the surface normal. The sample temperature was controlled by liquid helium during the measurements.

Figure 1 shows photoelectron spectroscopy (PES) spectra on cleaved SCG and MnPc/SCG taken at room temperature (RT) and ca. 10 K. Peak A is derived from Pc π-orbital as found for other MPcs. Peak B is uniquely observed for the MnPc as the highest occupied molecular orbital (HOMO) which is contributed strongly from Mn 3*d*-orbital. These peaks are shifted and become sharper at 10 K. Figures 2 (a-c) are the momentum maps at the energy of peak A (ΔE = 0.20 eV). In Fig. 2 (a), the intensity pattern from the SCG π-bands can be confirmed clearly. By adsorption of MnPc, the ring-like pattern along the π-bands of SCG at RT appeared (Fig. 2 (b)). On the other hand, the momentum map of MnPc/SCG at 10 K (Fig. 2 (c)) shows another intensity patterns with several lobes, where the faint ring-like pattern of the RT sample is superimposed. According to DFT calculations on MPc, the momentum map at HOMO shows the specific intensity patterns reflected C_{4v} symmetry [2]. Ring-like pattern suggests that π-orbital planes of the MnPc molecules are not ordered azimuthally on SCG at RT, then the several molecules make stable structure upon the cooling to give a specific lobe pattern. The presence of some disordered domains is indicated by the faint ring-like pattern at 10 K.

Additionally, another intensity pattern by six lobes appeared inside of the ring-like pattern at 10 K. Figures 2 (d-f) show band distribution maps corresponding to the momentum maps, respectively. In the distribution map of MnPc/SCG at 10 K (Fig. 2 (f)), another band dispersion can be confirmed inside of SCG π-bands and the value of k_x is coincident with the six-lobe pattern in the momentum map.

Since the interaction between MnPc and graphite is so weak [3], it is unlikely that a chemical change occurred between them. It is possible to consider that the appearance of band dispersion is due to phonon scattering at MnPc layers and derived from SCG π-bands. The reason for the appearance at 10 K may be due to the formation of oriented MnPc layers by cooling. These results lead to deeper understanding of weak molecule-substrate interactions.

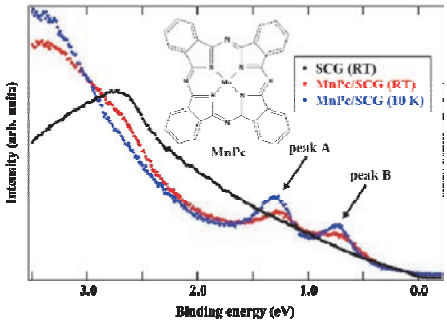

Fig. 1. Photoelectron spectra on the cleaved SCG and MnPc/SCG integrated over the whole angle. The structural formula of MnPc is shown in the inset.

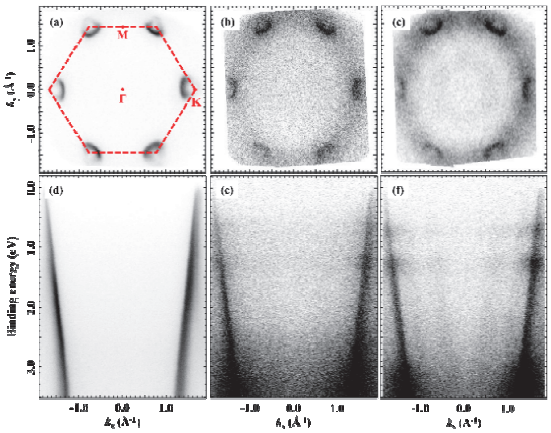

Fig. 2. (a-c): Momentum maps at peak A in Fig. 1. (a): Cleaved SCG and schematic image of hexagonal Brillouin zone. (b): MnPc/SCG at RT. (c): MnPc/SCG at 10 K. (d-f): Band distribution maps integrated over the range of k_y = (0.0±0.3) Å^{-1}. (d): Cleaved SCG. (e): MnPc/SCG at RT. (f): MnPc/SCG at 10 K.

[1] K. Nakamura *et al.*, Phys. Rev. B **85** (2012) 235129.
[2] D. Lüftner *et al.*, J. Elec. Spec. **195** (2014) 293.
[3] C. Isvoranu *et al.*, J. Chem. Phys. **131** (2009) 214709.

BL6U

Imaging the Domain Boundary of Ir(111) Thin Films by Momentum-selective PEEM Using Photoelectron Momentum Microscope

E. Hashimoto[1], H. Kurosaka[1], Y. Nishio[1], K. Hagiwara[2], F. Matsui[2] and S. Koh[1]

[1]*Department of Electrical Engineering and Electronics, College of Science and Engineering, Aoyama Gakuin University, 5-10-1 Fuchinobe, Chuo-ku, Sagamihara, Kanagawa 252-5258, Japan*

[2]*UVSOR Synchrotron Facility, Institute for Molecular Science, Okazaki 444-8585, Japan*

Iridium (Ir) is a transition metal belonging to the platinum elements group. Ir(111) is promising as a substrate for graphene growth by chemical vapor deposition (CVD). In addition, Ir(001) is used as a growth substrate for CVD diamond and a spin filter with high spin detection efficiency in spin-resolved photoemission spectroscopy. It is desired to establish methods for fabricating high quality Ir thin films at a few Å thick near the surface that can replace expensive bulk-single-crystals and methods for their characterization. In this study, we deposited Ir(111) thin films with high single-crystallinity by molecular beam epitaxy (MBE) and visualized the domain structure by momentum selective photoelectron emission microscopy (PEEM) using photoelectron momentum microscope [1,2].

We deposited Ir(111) thin films on α-Al_2O_3(0001) substrates by MBE method. First, the low-temperature buffer layer was deposited with the temperature of the substrate holder set at 500°C for 180 min. Then, the temperature of the sample holder was raised to 950°C, and the Ir(111) thin films were deposited for 120 min. By deposition for a total of 300 min, thin films with a thickness of 60 nm were grown. Afterwards, Ir(111) thin films were annealed under H_2 atmosphere at 1000°C for 60 min. Figures 1(a) and (b) show the XRD diffraction for the Ir layers on α-Al_2O_3(0001). Diffraction peaks caused by Ir(111) and α-Al_2O_3(0001) were observed in the $2\theta/\omega$ profile (Fig.1(a)). The XRD pole figure along Ir[111] is shown in Fig.1(b). The observed Bragg peaks displayed 6-fold symmetry, whereas the ideal Bragg peaks for Ir{111} exhibit 3-fold symmetry, thus indicating that Ir(111) contained twin domains.

Figures 2(a)-(c) show the band structures of Ir(111) thin films at Fermi energy by momentum-resolved photoelectron spectroscopy (MRPES). The field of view of MRPES is φ5 μm The photon energy was set to 100 eV. As shown in Fig. 2(a), we observed a 3-fold symmetry pattern of Ir. At the different measurement point 100 μm apart from the initial point, a 6-fold symmetry pattern corresponding to a domain boundary was observed (Fig.2(b)). With further movement of the measurement point, a 3-fold symmetry pattern rotated by 180 degrees from the 3-fold symmetry pattern at the initial point was observed (Fig.2(c)).

Momentum-selective PEEM images were acquired by inserting the contrast aperture into momentum space with the strongest photoelectron intensity in the MΓM direction ($E = E_F$ - 1 eV, $k_x \simeq 0$ Å^{-1}, $k_y \simeq 1$ Å^{-1}, in Fig. 2(a)). Without inserting the aperture, the PEEM image without contrast was obtained, which did not reflect the domain structure, as shown in Fig.3(a). In Fig. 3(b), when the aperture was inserted, we observed that the bright region corresponded to the domain with band structure, as shown in Fig.2(a). On the contrary, when an aperture is inserted in the domain with Fig. 2(c), a PEEM image with inverted contrast can be imaged, as shown in Fig. 3(c). Repeating similar PEEM measurements in different regions, found that unidirectional domains exist over several hundred μm × several hundred μm. We successfully observed twin-domain structures with no chemical shifts and only geometric differences in band structure using momentum-selective PEEM measurements.

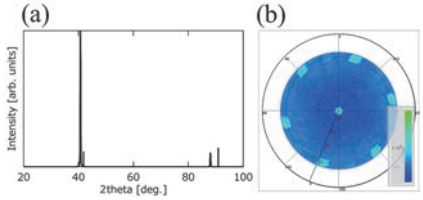

Fig. 1. (a) 2θ/ω profile and (b) pole figure of Ir(111) thin films deposited by MBE.

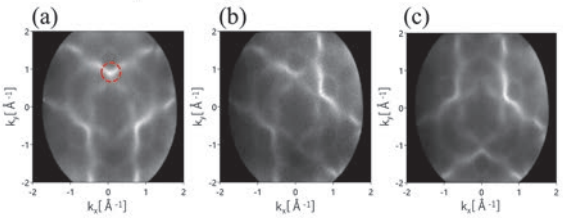

Fig. 2. The band structures of Ir(111) at Fermi energy. The observation point of (b) was moved 100 μm from (a), and (c) was moved 100 μm from (b).

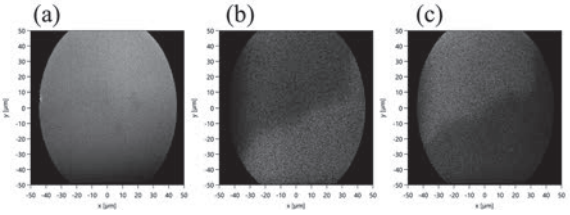

Fig. 3. PEEM images of Ir(111) thin films. (a) without inserting aperture, (b) and (c) with inserting aperture.

[1] F. Matsui *et al*., J. Phys. Soc. Jpn. **91** (2022) 097403.
[2] F. Matsui *et al*., Rev. Sci. Instrum. **94** (2023) 083701.

III-4